*Ecology Letters*, (2008) **11**: 128–138 doi: 10.1111/j.1461-0248.2007.01131.x

LETTER

# Leading indicators of trophic cascades

**S. R. Carpenter,[1]* W. A. Brock,[2] J. J. Cole,[3] J. F. Kitchell[1] and M. L. Pace[3]**
[1]*Center for Limnology, University of Wisconsin, Madison, WI 53706, USA*
[2]*Department of Economics, University of Wisconsin, Madison, WI 53706, USA*
[3]*Institute of Ecosystem Studies, PO Box AB, Millbrook, NY 12545, USA*
**Correspondence: E-mail: srcarpen@wisc.edu*

## Abstract

Regime shifts are large, long-lasting changes in ecosystems. They are often hard to predict but may have leading indicators which are detectable in advance. Potential leading indicators include wider swings in dynamics of key ecosystem variables, slower return rates after perturbation and shift of variance towards lower frequencies. We evaluated these indicators using a food web model calibrated to long-term whole-lake experiments. We investigated whether impending regime shifts driven by gradual increase in exploitation of the top predator can create signals that cascade through food webs and be discerned in phytoplankton. Substantial changes in standard deviations, return rates and spectra occurred near the switch point, even two trophic levels removed from the regime shift in fishes. Signals of regime shift can be detected well in advance, if the driver of the regime shift changes much more slowly than the dynamics of key ecosystem variables which can be sampled frequently enough to measure the indicators. However, the regime shift may occur long after the driver has passed the critical point, because of very slow transient dynamics near the critical point. Thus, the ecosystem can be poised for regime shift by the time the signal is discernible. Field tests are needed to evaluate these indicators.

## Keywords

Alternate stable state, depensation, lake, leading indicator, return rate, spectrum, stochastic differential equations, threshold, trophic cascade, variance.

*Ecology Letters* (2008) 11: 128–138

## INTRODUCTION

Most ecological change is gradual and incremental, but sometimes extensive changes occur in ecosystems over short periods of time (Holling 1973; Scheffer *et al.* 2001; Carpenter 2003; Walker & Meyers 2004). Massive changes may involve nonlinear dynamics, thresholds and cross-scale interactions. The generic term 'regime shift' represents this diverse class of big changes (Carpenter 2003; Scheffer & Carpenter 2003; Scheffer & Jeppesen 2007). Regime shifts are known for a wide variety of ecological systems including marine ecosystems (Simenstad *et al.* 1978; Steele 1998; Walters & Kitchell 2001), spatial dynamics of vegetation (Peters *et al.* 2004; Rietkerk *et al.* 2004), drylands (Reynolds & Stafford-Smith 2002; Foley *et al.* 2003), managed rangelands (Anderies *et al.* 2002), succession and restoration in terrestrial plant communities (Suding *et al.* 2004; Schmitz *et al.* 2006) and lakes (Scheffer 1997; Jeppesen *et al.* 1998; Carpenter 2003). Mechanisms of regime shifts are also diverse, involving, for example, feedbacks between vegetation and the atmosphere (Foley *et al.* 2003; Narisma *et al.* 2007), soil (Rietkerk *et al.* 2004) or fire (Peters *et al.* 2004); biogeochemical feedbacks (Carpenter 2003) or complex interactions in food webs (Scheffer 1997; Jeppesen *et al.* 1998; Schmitz *et al.* 2006; Persson *et al.* 2007).

An important class of regime shifts involves transitions among alternate states in food webs (Ives & Carpenter 2007). The transitions can be driven by gradual change in exploitation of a top predator or prey species, reintroduction of a predator or modification of habitat (Walters & Kitchell 2001; Schmitz *et al.* 2006; Persson *et al.* 2007). In these regime shifts, gradual change of a driver (such as predator removal or habitat modification) leads to abrupt reorganization of the ecosystem. Analogous situations exist in atmosphere–land or atmosphere–ocean interactions where gradual climate warming can lead to abrupt changes in weather or ocean currents (Berglund & Gentz 2002; Foley *et al.* 2003; Kleinen *et al.* 2003). In this paper, we focus on ecological regime shifts driven by gradual changes in harvest of a predator, a phenomenon known from field studies of both aquatic and terrestrial ecosystems (Schmitz *et al.* 2006; Persson *et al.* 2007).

Regime shifts are difficult to predict or anticipate (Clark *et al.* 2001). Routine, incremental change is a poor baseline

for forecasting unusual changes that extend beyond the range of historical experience (Carpenter 2002, 2003). Thresholds are rarely known before they are crossed (Groffman *et al.* 2006). The limited capacity to anticipate regime shifts is a significant problem for ecosystem management, especially because reversals may be difficult, expensive or in some cases, impossible (Folke *et al.* 2005). However, the capacity to anticipate or forecast regime shift would be extremely valuable because dramatic changes can often lead to large losses of ecosystem services with severe consequences for human well-being (MA (Millennium Ecosystem Assessment) 2005).

Theory suggests that some variables within ecosystems do change before regime shifts in ways that may serve as leading indicators of change. Specifically for time series observations of ecosystem state variables such as biomasses or chemical concentrations, standard deviations may increase (Carpenter & Brock 2006), variance may shift to lower frequencies in the variance spectrum (Kleinen *et al.* 2003) and return rates in response to disturbance may decrease (van Nes & Scheffer 2007) prior to a change.

To illustrate these ideas more precisely, consider the simple case of a one-dimensional system $x$ with rate of change $dx/dt$ shown as the solid line in Fig. 1. Dynamics of $x$ depend on a driver variable which changes gradually from panels A through D of Fig. 1, moving the solid curved line downward from panel to panel. In Fig. 1a, there are three equilibria where $dx/dt = 0$ (circles). The black and grey equilibria are stable because small perturbations of $x$ to the left or right lead to positive or negative rates, respectively, moving $x$ back towards the equilibrium. The white circle is an unstable equilibrium because small perturbations of $x$ to the left or right lead to negative or positive rates, respectively, moving $x$ away from the white equilibrium. As the driver variable moves the solid curve downward, the grey stable point becomes less resilient (closer to the unstable point) in Fig. 1b, coalesces with the unstable point in Fig. 1c and disappears altogether in Fig. 1d.

To this familiar graphical analysis of stability we now add the idea of small random shocks to the rate, $dx/dt$. Consider dynamics near the grey stable point. In Fig. 1a, perturbations are damped rather rapidly due to the steep slope of the solid line near the grey equilibrium. The return rate is relatively fast, the variance of $x$ is relatively small and the variance spectrum is relatively 'white' (i.e. variance is distributed rather evenly across the range of frequencies). A variance spectrum breaks the total variance of $x$ into components of different frequencies, summarized as a plot of variance vs. frequency (Fortin & Dale 2005). In Fig. 1b, the slope of the solid line near the grey equilibrium is flatter. Return rate is slower, variance of $x$ is higher, and the variance spectrum becomes more pink (i.e. lower frequencies become more important). In Fig. 1c, the grey and white equilibria coalesce and the slope of the solid line is zero at the equilibrium which is white to denote its lack of stability. The return rate from small perturbations is near zero, the variance of $x$ is large, and the variance spectrum becomes even redder as lower frequencies become even more important. To complete the regime shift, in Fig. 1d only the black equilibrium remains. Return rate is again rather fast, variance of $x$ is rather low, and the spectrum is rather white. For a mathematical explanation of these changes see Kleinen *et al.* (2003), Carpenter & Brock (2006) and van Nes & Scheffer (2007).

While regime shift indicators are promising tools for understanding and management, these indicators are known

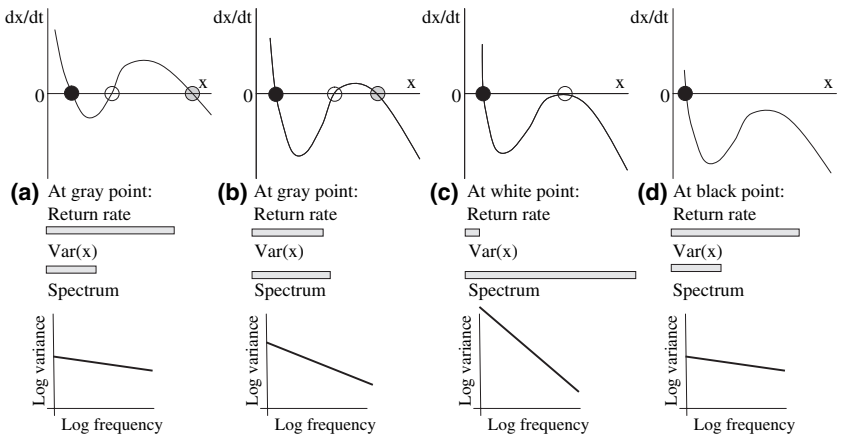


**Figure 1** Changes in stability at different levels of a driving variable. Each panel shows the rate of change in $x$, $dx/dt$, vs. $x$. From panels (a–d) a driving variable is changed causing one stable equilibrium of $x$ to disappear. Labels under each panel explain the qualitative changes in return rate, variance of $x$ and variance power spectrum of $x$. (a) Two stable equilibria (black and grey) and an unstable equilibrium (white). (b) Two stable equilibria but the grey stable point is closer to the unstable white point. (c) Gray stable equilibrium has disappeared. (d) White unstable equilibrium has disappeared.

primarily from theory, physical systems and a few models for ecosystems. Exploring these indicators under realistic ecological conditions where regime shifts are known to occur provides a means to further evaluate the potential of this approach. Alternate states in fish communities are well known (e.g. Walters & Kitchell 2001; Carpenter 2003; Persson *et al.* 2007) and provide a test case. Regime shifts in lake food webs are particularly interesting, in part, because there are instruments that can make high frequency measurements of aquatic biota and chemistry providing the time series needed to test for indicators. However, variance effects of a regime shift might not be detectable when mixed with other sources of variance that impact populations within complex food webs. For example, variance because of an impending regime shift could be attenuated as it passes through a food web or drowned out by other sources of variance.

The arguments above suggest that it is not clear whether regime shift indicators will be detectable in multiple components of a food web subject to multiple sources of noise. To investigate this possibility, we conducted a model analysis of regime shift indicators using a food web model based on whole lake manipulations of nutrients and top predators. In the model we manipulated harvest of the top predator until a regime shift occurred, driven by cascading trophic interactions. The bifurcation that creates the regime shift results from changes in predation by piscivores and refuge use by planktivores. This shift cascades to the zooplankton and phytoplankton. We use the model to calculate the three indicators – time series standard deviations, return rates from disturbance and variance spectra – for planktivores, zooplankton and phytoplankton before, during and after the regime shift. We also used a multivariate index of variability for the food web. In our simulations, we added independent noise to planktivores, herbivores and phytoplankton to test whether regime shifts could be discerned in the presence of variability that was unrelated to the regime shift. We were particularly interested in responses of the phytoplankton because they can be observed at high frequency using modern sensors and could be useful indicators of regime shifts under field conditions. Thus, the model analysis provides a test of the efficacy of regime shift indicators under realistic conditions drawn from prior field experiments.

## METHODS

To evaluate the indicators in a food web context with multiple sources of variance, we used a model for the food web in the epilimnion of a lake (Fig. 2). We have determined the responses of such food webs to nutrient and predator manipulations in a series of whole-lake experiments from 1984 to 1997 (Carpenter & Kitchell 1993; Carpenter *et al.* 2001). The food web involves a trophic triangle of two size classes of piscivorous fish (adult and juvenile) and a planktivorous fish which preys on juvenile piscivores as well as herbivorous zooplankton (Ursin 1982; Walters & Kitchell 2001). The herbivores, in turn, feed on phytoplankton. Phytoplankton growth depends on irradiance and phosphorus input rate. Planktivores and juvenile piscivores move between the open water habitat and refuges such as littoral habitat. Herbivores can migrate between the epilimnion and a deep-water refuge. Thus, our model combines predator–prey interactions and movement between refugia and foraging arenas (Walters & Martell 2004).

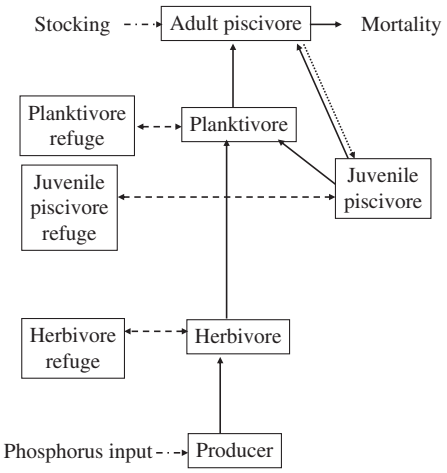


**Figure 2** Compartments and feedbacks for the food web model explained in the text. Producers are phytoplankton, which are affected by phosphorus input. Herbivores are zooplankton, which consume phytoplankton, are consumed by planktivores, and can migrate in or out of a refuge. Planktivores are fishes which consume herbivores and juvenile piscivores, are preyed upon by adult piscivores, and have access to a refuge. Juvenile piscivores are produced by adult piscivores, are consumed by planktivores and adult piscivores, and have access to a refuge. Adult piscivores consume both planktivores and juvenile piscivores, and are subject to both stocking and harvest mortality.

### Model Description

Fish components of the model are solved on two time scales, the time interval for juvenile piscivores to mature to adults (referred to as the maturation interval) and the much shorter time step between instantaneous random shocks to the state variables.

Within one maturation interval, dynamics of the fishes are:

$$\frac{\mathrm{d}A}{\mathrm{d}t} = -qEA \qquad (1)$$

$$\frac{dF}{dt} = D_F(F_R - F) - c_{FA}FA + \sigma_F \frac{dW_F}{dt} \quad (2)$$

$$\frac{dJ}{dt} = -c_{JA}JA - \frac{c_{JF}vFJ}{h + v + c_{JF}F} \quad (3)$$

$A$ is adult bass, $F$ is the planktivore, $J$ is juvenile bass. Parameters are: catchability ($q$), effort ($E$), exchange rate of $F$ between the foraging arena and a refuge ($D_F$), refuge reservoir of $F$ ($F_R$), consumption rate of $F$ by $A$ ($c_{FA}$), additive noise ($\sigma_F$), Wiener stochastic process ($dW/dt$), control of $J$ by $A$ ($c_{JA}$), consumption rate of $J$ by $F$ ($c_{JF}$), rate at which $J$ enter the foraging arena ($v$), rate at which $J$ seek refuge ($h$). The harvest rate referred to in the main text is the product $qE$. Symbols, units and parameter values are shown in Table S1.

Prey fishes are assumed to move between refugia and a foraging arena (Walters & Martell 2004). Planktivores move between the pelagic zone ('inside' the model) and a refuge which is not explicitly modelled and is assumed to sustain a population of planktivores. In reality, the refuge could represent an area inaccessible to piscivores, or another aquatic system connected to the lake in the model. Similarly, juvenile piscivores move between an open-water foraging arena and a refuge that is inaccessible to planktivores (Walters & Martell 2004).

Equations 1–3 address population dynamics not somatic growth, so predation counts as a loss to the victim population but not as an increment to the predator population.

At the beginning of each maturation interval, a cohort of $J$ is spawned. Then numbers decline due to predation, and survivors recruit to the $A$ pool the following maturation interval. The pseudocode is:

(1) obtain initial values: $A_t$, $F_t$, $J_t$;
(2) integrate eqns 1–3 over one maturation interval to compute $A_{t+i}$, $F_{t+i}$, $J_{t+i}$, where the subscript $t + i$ means 'integrated from $t$ to the end of one maturation interval';
(3) compute the initial conditions for maturation interval $t + 1$. Survivorship from the end of maturation interval $t$ to the beginning of maturation interval $t + 1$ is $s$. Juveniles that survive become adults. Production of juveniles per adult is $f$ at the beginning of maturation interval $t + 1$ and

$$A_{t+1} = s(A_{t+i} + J_{t+i}) \quad (4)$$

$$F_{t+1} = F_{t+i} \quad (5)$$

$$J_{t+1} = fsA_{t+1} \quad (6)$$

(4) then repeat steps 1–3 for successive maturation intervals.

The planktivore $F$ and the inputs of the limiting nutrient control the plankton. The zooplankton dynamics are

$$\frac{dH}{dt} = D_H(H_R - H) + \alpha c_{HP}HP - c_{HF}HF + \sigma_H \frac{dW_H}{dt} \quad (7)$$

$D_H$ is exchange rate of herbivores from a refuge (e.g. the hypolimnion) which supports density $H_R$. The zooplanktivory rate coefficient is $c_{HF}$. Noise is added by a Weiner stochastic process with standard deviation $\sigma_H$.

The phytoplankton dynamics are

$$\frac{dP}{dt} = r_P L\gamma(I_0, P)P - mP - c_{PH}HP + \sigma_P \frac{dW_P}{dt}, \quad (8)$$

where $r_P$ is a growth parameter for phytoplankton, $L$ is phosphorus loading rate, $m$ is a non-predatory mortality (sinking) rate and $c_{PH}$ is the grazing rate coefficient. Noise is added by a Weiner stochastic process with standard deviation $\sigma_P$. The light function $\gamma$ is based on the model of Dutkiewicz *et al.* (2005) and Follows *et al.* (2007):

$$\gamma(I_0, P) = \int_0^{Z_{mix}} \frac{1}{F_{max}} \left[\left(1 - \exp(-k_{grow}I(Z,P))\right) \exp(-k_{inhib}I(Z,P))\right] dZ$$

$$I(Z,P) = I_0 \exp[-Z(k_o + k_{DOC}DOC + k_P P)]$$

$$F_{max} \equiv \frac{k_{grow} + k_{inhib}}{k_{grow}} \exp\left(-\frac{k_{inhib}}{k_{grow}} \ln\left(\frac{k_{inhib}}{k_{grow} + k_{inhib}}\right)\right) \quad (9)$$

The mixed layer depth is $z_{mix}$. Irradiance has a positive effect on growth through the parameter $k_{grow}$, and an inverse effect at high irradiance levels through the parameter $k_{inhib}$. Light is attenuated by absorption by water ($k_o$), dissolved organic carbon ($k_{DOC}$) and phytoplankton biomass ($k_P$). $F_{max}$ is a normalization constant that causes the maximum value of $\gamma(I_0,P)$ to be 1.

## Simulations

Model parameters (Table S1) were taken from the literature or adjusted to match summer average biomasses observed during whole-lake experiments that manipulated the dominant fishes (piscivores or planktivores) or nutrient loading (Carpenter & Kitchell 1993; Carpenter *et al.* 2001). We did not formally fit the model using statistical procedures. We adjusted parameter values until steady-state biomasses of all state variables were similar to summer average biomasses for each food web configuration and nutrient input rate studied in the experiments. Although the historical data are adequate for calibrating the model, they lack the temporal resolution needed to evaluate the regime-shift indicators. Our goal here was to evaluate the indicators in a model context, as a first step towards designing experiments to evaluate the indicators in the field.

The goal of this paper was to investigate the transmission of random disturbances through the food web, and whether variance related to a regime shift can be discerned against a background of other variance unrelated to the regime shift. The regime shift is created by gradually increasing harvest rate of adult piscivores, the parameter $qE$ in the model which stands for the product of catchability and effort (Table S1). Eventually, a critical harvest rate is reached where piscivory on planktivores is no longer able to control predation by the planktivores on the juvenile piscivores (Walters & Kitchell 2001; Carpenter & Brock 2004). Piscivore recruitment is thereby shut off, and the ecosystem shifts from piscivore dominance to planktivore dominance. The herbivores and phytoplankton change because of a trophic cascade which is triggered by the nonlinear dynamics of the fishes.

As harvest of the top predator increases, can variability measured in lower trophic levels signal an impending regime shift in the fishes, despite multiple sources of noise in the ecosystem? To address this question, we added random disturbances to the dynamics of the planktivore, which is a key species in the regime shift, as well as to the dynamics of the herbivore and the phytoplankton. The herbivore and the phytoplankton are not involved directly in the regime shift, but are indirectly affected by the resulting trophic cascade. Thus, we could investigate whether the signal of the regime shift could be discerned in the herbivore and phytoplankton dynamics despite the addition of unrelated noise to the system.

We measured stationary distributions of the ecosystem components at different levels of harvest rate. We also examined transient simulations in which harvest rate was slowly increased over a long period of time.

Stationary distributions were studied by a three-stage process for each level of harvest rate. (i) Steady states of the deterministic skeleton of the model were estimated by numerical optimization (Appendix S1). (ii) Stochastic simulations were initiated near the steady state of the deterministic skeleton and run for 5120 time steps. Time series were inspected graphically to ensure that they appeared stationary. (iii) Samples from the stationary distribution were collected for an additional 2048 time steps.

Transient time series were studied by slowly and gradually increasing the harvest rate during simulations. The goal was to increase the harvest rate slowly relative to the time scale of the random disturbances and the dynamics of the food web. Simulations were initiated near the steady state of the deterministic skeleton of the model. The harvest rate was increased from 1.5 to 2.0 linearly across 96 000 time steps. This length of simulation changes the harvest rate slowly enough, and is a convenient multiple of the maturation interval. In the deterministic skeleton of the model, the high-biomass steady state of the piscivore disappears when the harvest rate is *c.* 1.716 (Appendix S1). Thus, the harvest rate crossed this critical value during the simulation.

Four potential indicators of regime shift were calculated for the simulation results: (i) the standard deviation of the state variables, (ii) a multivariate index of variability of the food web as a whole, (iii) an estimate of return rate for the state variables and (iv) spectra of the state variables. The multivariate index is the square root of the dominant eigenvalue of the covariance matrix of the state variables (Brock & Carpenter 2006). The return rate was estimated by fitting the univariate autoregression model $x_{t+1} = b_0 + b_1 x_t + \varepsilon_t$, where $x$ is the time series of the state variable, $b_0$ and $b_1$ are parameters estimated by least squares and $\varepsilon_t$ is a time series of errors. Then $1/b_1$ is an estimator of return rate (Ives *et al.* 2003). Spectral analyses were computed by Fourier analysis of the time series using the 'spectrum' command in R.

The system of equations was solved by the Euler method using Ito calculus (Horsthemke & Lefever 1984). For results shown in this paper, we used 32 small time increments per maturation time. We experimented with 64 and 128 increments per maturation time and obtained nearly identical results. All computations were performed in R (http://www.r-project.org/).

## RESULTS

Statistics for the stationary distributions of the stochastic state variables (planktivore, herbivore and phytoplankton biomass) are presented across a gradient of the harvest rate, $qE$ (Fig. 3). Steep changes in the means of the stationary distributions occur for values of $qE$ between *c.* 1.70 and 1.72 (Fig. 3a,d,g). For the deterministic skeleton of the model (i.e. the model with all stochastic disturbances set to zero), the switch point where the piscivores' high-biomass stable equilibrium vanishes is near $qE = 1.716$ (Appendix S1). The stochastic version of the model appears to shift regimes near the same value of $qE$ as the deterministic skeleton.

The standard deviations of all stochastic state variables increase substantially near the switch point near $qE = 1.716$ (Fig. 3b,e,h). Note the logarithmic $y$-axis. The increase in standard deviation is *c.* 20-fold for the planktivore (Fig. 3b), threefold for the herbivore (Fig. 3e) and 10-fold for the phytoplankton (Fig. 3h). Initially, the rise in standard deviation is related to declining stability of the state variables as $qE$ rises. Eventually $qE$ is large enough that some data points jump towards the alternative attractor. As $qE$ rises still farther, there are some data points in each of the stable states. Eventually, the data points are mostly near the new attractor, and then at high $qE$ the data points are all near the new attractor. This sequence is reflected in flattening of the stationary distributions and separation into bimodal distributions near the switch point (Figs S1–S4).

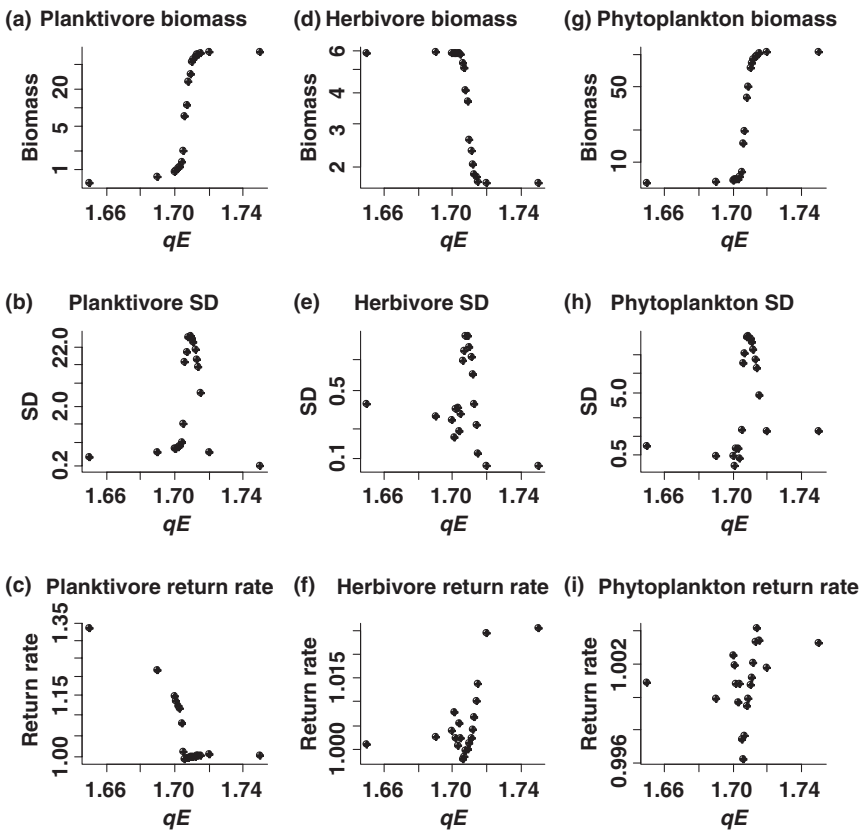


**Figure 3** Statistics for the stationary distributions of planktivore (left column), herbivore (middle column) and phytoplankton (right column) across a gradient of $qE$: mean (top row), standard deviation (middle row) and return rate (bottom row).

Return rate, estimated from time series output using the method of Ives *et al.* (2003), decreases substantially near the switch point near $qE = 1.716$ (Fig. 3c,f,i). A return rate of 1.0 indicates that the system does not return from a small perturbation. Return rates > 1.0 indicate that the system returns exponentially to equilibrium after a small perturbation, while return rates < 1.0 indicate that the system diverges after a small perturbation. The planktivore return rate is *c.* 1.0 near the switch point, indicating lack of recovery from a small perturbation, and > 1.0 for $qE$ values away from the switch point, indicating exponential return to equilibrium following small perturbations (Fig. 3c). The herbivore return rate is slightly above 1.0 at $qE$ values below and above the switch point, indicating exponential return to equilibrium after perturbation (Fig. 3f). Near the switch point, herbivore return rates are slightly below 1.0, indicating a tendency to diverge from equilibrium after small perturbations. Divergence is reflected in the bimodal stationary distributions of the herbivore at some values of $qE$ near the switch point (Fig. S3). The phytoplankton, like the herbivore, has return rates slightly above 1.0 except near the switch point when phytoplankton return rates are slightly < 1.0 (Fig. 3i). The divergence suggested by these return rates is consistent with the bimodal stationary distributions seen for phytoplankton at some values of $qE$ near the switch point (Fig. S4).

The multivariate index rises sharply near the switch point near $qE = 1.716$, but is relatively flat otherwise (Fig. 4). The increase near the switch point is *c.* 50-fold.

Variance spectra of phytoplankton were computed for the same values of $qE$ used in Figs 3 and 4. At a fixed value of $qE$, spectral analysis yields a plot of variance (or spectral density) vs. frequency (cycles per unit time). Both the variance and frequency axes are log-transformed to envision their relationship more clearly. We combined the spectra from all the values of $qE$ in a contour plot (Fig. 5). The contours are log-transformed variance, or spectral density. The *x*-axis is log frequency in cycles per sample interval; one maturation interval = −3.47 [there were 32 samples per maturation interval, and log (1/32) = −3.47]. The *y*-axis is $qE$.

Near the switch point at $qE = 1.716$, variance at low frequency rises sharply to a plateau (Fig. 5). The plateau appears as the white area between $qE$ of *c.* 1.7 and 1.72, and frequency lower than *c.* −5.5. At high frequencies (above about −5) variance sometimes declines, suggesting a flow of variance from high frequencies to low frequencies. Each black contour line in Fig. 5 represents a change in variance of two natural logs. The variance plateau is about four contours (eight natural logs), or *c.* 3000-fold, above the surrounding terrain. Similar variance plateaus appear in the spectra for the herbivore (Fig. S5) and planktivore (Fig. S6).

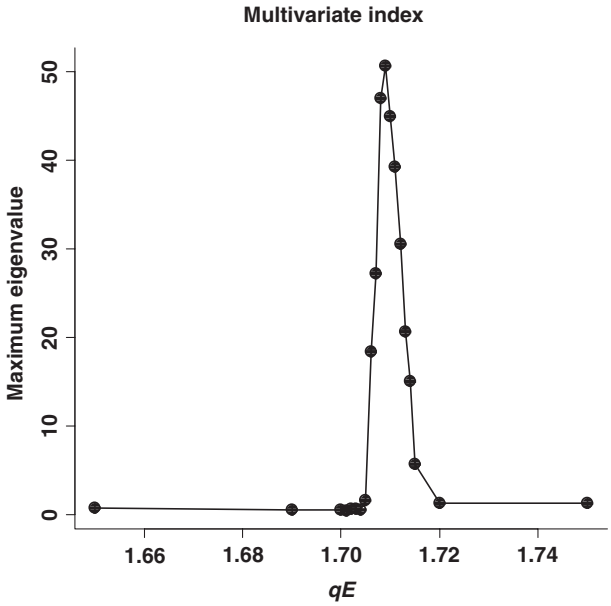


**Figure 4** Multivariate index (maximum eigenvalue of the covariance matrix of state variable biomasses) vs. harvest rate $qE$ in the stationary simulations.

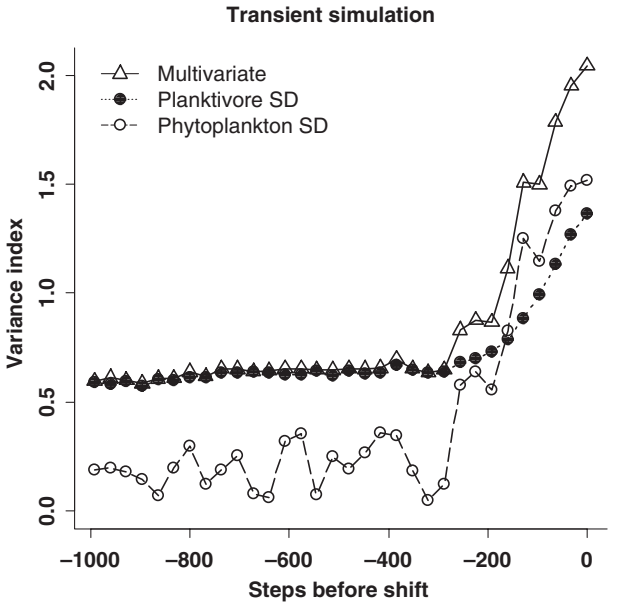


**Figure 6** Indicators vs. time steps prior to regime shift: multivariate index (open triangles, solid line), standard deviation of the planktivore (dark circles, dotted line) and standard deviation of the phytoplankton (open circles, dashed line).

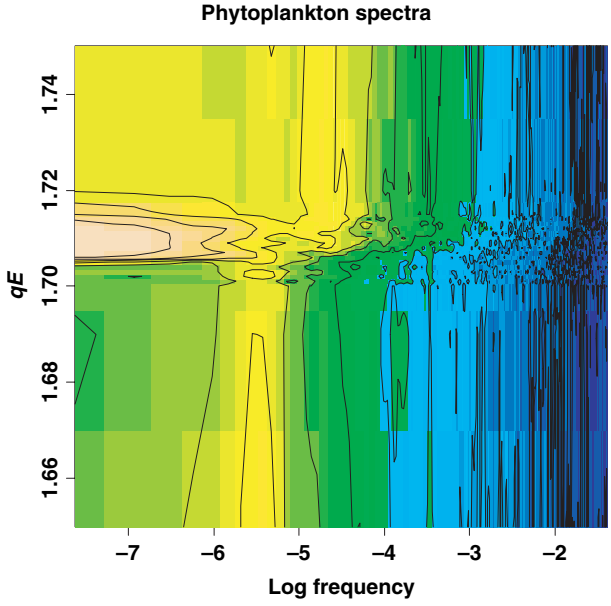


**Figure 5** Log spectral density (contours) vs. log frequency [horizontal axis; log(one maturation interval) = −3.47] and $qE$ (vertical axis) for planktivore biomass. Colours correspond with a topographic map; starting with the lowest spectral density in blue, log spectral density rises from −11 to +11 through green, yellow, dark tan and light tan as the highest spectral density.

In field studies, it is usually impossible to observe stationary distributions so indicators of ecosystem dynamics must be derived from observations of non-stationary time series. Results from a transient simulation are illustrated in Fig. 6. Statistical indicators were computed for each maturation interval (32 samples) prior to the shift between piscivore dominance and planktivore dominance. Numerically, we defined the regime shift as the time step with most rapid change in the planktivore biomass. The standard deviation of the planktivore and the phytoplankton, and the multivariate index, rise steeply prior to the shift in fish dominance, and the rise starts *c.* 200 time steps (six or seven maturation intervals) before the shift in fish dominance. However, the standard deviation of the juvenile planktivore decreases prior to the shift, while the standard deviation of the herbivore is noisy and hard to interpret (Fig. S7; note log $y$ axes).

Changes in return rate in the transient simulations were also complex (Fig. S8). The planktivore return rate declined from *c.* 500–200 samples before the shift, and then rose sharply. The juvenile piscivore return rate rose steadily up to the switch. The herbivore return rate was noisy and hard to interpret. The same was true of the phytoplankton return rate until *c.* 300 time steps before the shift. Then, the phytoplankton return rates clustered near 1.0.

It is important to note that in the transient simulations $qE$ passed the switch point for the deterministic skeleton of the model (near $qE = 1.716$) long before the shift in fish dominance. In the simulation illustrated in Fig. 6, $qE$ reached the switch point for the deterministic skeleton 9247 time steps (*c.* 290 maturation times) before the shift in fish

populations, far earlier than results shown in the graph. There were no discernible changes in the time series when $qE$ passed the switch point. The big changes in the time series occurred in the last 200 or so time steps before the shift in fish dominance.

## DISCUSSION

Regime shifts are large and often important changes in ecosystems, with long-lasting consequences. Examples include rangeland degradation (Anderies *et al.* 2002), replacement of coral reefs by attached algae (Hughes *et al.* 2005), multiple trajectories of secondary succession (Schmitz *et al.* 2006), abrupt shifts in fish communities (Persson *et al.* 2007), clear-water and turbid phases in shallow lakes (Scheffer & Jeppesen 2007) and many others (Walker & Meyers 2004). Yet regime shifts are often hard to predict, and often come as surprises (MA (Millennium Ecosystem Assessment) 2005). For regime shifts associated with certain kinds of nonlinear changes in ecosystems, observed time series should change in discernible ways before the regime shift occurs. These changes include increases in variance of species abundances or biomasses of entire trophic levels (and multivariate combinations of these variances), slower return rates from small perturbations and a shift of variance spectra towards lower frequencies (Kleinen *et al.* 2003; Brock & Carpenter 2006; Carpenter & Brock 2006; van Nes & Scheffer 2007). These changes occur as the original ecosystem state becomes less stable. Therefore, they are leading indicators of impending regime shift. The changes intensify as the ecosystem transitions between the alternate states, and then drop to lower values if the new state becomes more stable.

We evaluated these potential indicators using a simulation model of lakes subject to alternate states and trophic cascades, and calibrated to data from long-term whole-lake experiments. In the simulated stationary distributions, the indicators respond as expected from existing theory for ecosystem regime shifts near the critical harvest rate of the piscivore population. We observed increases in standard deviation, low return rates and steeper variance spectra with high plateaus of variance at lower frequencies. The increases in standard deviation and spectral shifts were especially pronounced. Thus, in stationary simulations, the variance signal of the fish regime shift was transmitted through the food web and detected in lower trophic levels. The signal was easily detectable in lower trophic levels despite the addition of noise unrelated to the regime shift.

In the stationary distributions, the sharpest response of the indicators is close to the switch point. These are 'leading indicators' in the sense that they change before harvest rate reaches the switch point. For example, there is an exponential increase in standard deviations of planktivore and phytoplankton as harvest rate rises towards the switch point, even rather far from the switch point. Much closer to the switch point, the exponential rise in standard deviation becomes sharply steeper. Though these changes are easily seen in stationary distributions, in practice an ecosystem manager must deal with non-stationary time series.

In transient simulations with slowly rising harvest rate, we observed large and consistent changes in some but not all of the indicators prior to the regime shift. Standard deviations of planktivores and phytoplankton were consistent with expectations, while the standard deviation of the juvenile piscivores declined as they became rare and the standard deviation of the zooplankton was noisy. The multivariate index seemed to overcome these inconsistencies. It was sensitive to the regime shift and was not confounded by unrelated noise, consistent with the findings of Brock & Carpenter (2006) in the context of a spatial model of ecosystem services. Return rates were more difficult to interpret in the transient simulations. In models, return rates can be estimated using the eigenvalues of linearized dynamics near equilibrium (van Nes & Scheffer 2007). Because our goal was to mimic observation of an ecosystem, we used a statistical estimator of return time appropriate for field data (Ives *et al.* 2003). Although both ways of estimating return time are based on similar ideas, they are not likely to give identical answers. In field data, the time interval used to estimate return rate (Ives *et al.* 2003) may affect the behaviour of the estimated return rate as the ecosystem move towards a regime shift. Through further research, it may be possible to choose time intervals that optimize the behaviour of return rate estimates in the context of leading indicators of regime shifts.

Fishing has been shown to increase variability in exploited fish stocks (Carpenter & Kitchell 1993; Mullon *et al.* 2005; Hsieh *et al.* 2006), and the greater variability in fish abundance cascades to lower trophic levels (Kitchell & Carpenter 1993). These phenomena have been explained by mechanisms different from the one explored in this paper. Nonetheless, the field observations are consistent with behaviour of the indicators investigated here and suggest that mechanisms should be investigated further.

The clear responses of the phytoplankton indicators are particularly interesting. Technology exists to make high-frequency measurements of phytoplankton production and pigment concentrations, ecosystem respiration and some chemical variables in pelagic systems (Porter *et al.* 2005). Our results indicate that changes in phytoplankton time series can signal regime shifts in fish populations long before they occur, even in transient simulations with added noise.

Changes seen in manipulations of piscivore populations in whole lakes suggest testable ecological mechanisms for the indicators seen in the model. As piscivore populations

decline, the risks and benefits to planktivorous fishes of foraging in refuge vs. offshore habitats should change. Thus, habitat use and diets of planktivorous fishes should become more variable as a wider range of habitats is exploited. Fish predation on larger-bodied zooplankton should gradually increase, leading to an increase in diel vertical migration and changes in community structure as smaller-bodied zooplankton become more abundant. Thus, zooplankton abundance in pelagic waters should become more variable because of migratory behaviour and changing composition. The shifts in zooplankton body size distribution, species composition and behaviour should lead to variability in grazing and nutrient recycling that affect the phytoplankton. These general patterns, known from many whole-lake piscivore manipulations, suggest that interesting changes in variance, return times and spectra may occur, and therefore that the idea merits further study in field experiments.

On the other hand, there are important reasons for caution. We have evaluated the indicators for the case of a regime shift in which one of the attractors disappears. This type of model has been applied to many ecological regime shifts (Holling 1973; Scheffer 1997; Scheffer *et al.* 2001; Carpenter 2003), but many other kinds of regime shifts may occur in ecosystems (Solé *et al.* 1996; Foley *et al.* 2003; Kleinen *et al.* 2003; Rietkerk *et al.* 2004; Walker & Meyers 2004; Groffman *et al.* 2006; Schmitz *et al.* 2006; Ives & Carpenter 2007; Narisma *et al.* 2007; van Nes & Scheffer 2007; Persson *et al.* 2007). The indicators may work in many of these cases but with only a few exceptions the necessary studies have not yet been conducted (Berglund & Gentz 2002; Kleinen *et al.* 2003; Brock & Carpenter 2006; Carpenter & Brock 2006; van Nes & Scheffer 2007). Thus, the indicators need to be evaluated in a wider variety of ecological settings. Also, additional kinds of indicators, such as spatial variance or covariance of ecological patterns, should be investigated. Finally, it is important to note that the sensitivity of the indicators depends on the time scales of change (in drivers, ecosystem components and frequency of random shocks) and the magnitude of disturbance. The particular ranges of conditions that make it possible to detect leading indicators may depend on the type of ecosystem and type of regime shift under study.

The indicators provide an advance warning only if the harvest rate is rising slowly in comparison with the dynamics of the ecosystem components and the random shocks. The studies performed so far indicate that warning signals can be discerned if the change in drivers is slow enough, but the specific value of 'slow enough' depends on the details of each specific case (Berglund & Gentz 2002; Kleinen *et al.* 2003; Brock & Carpenter 2006; Carpenter & Brock 2006; van Nes & Scheffer 2007). In the model presented here, if harvest rate increases too fast then the ecosystem will move across the switch point before the warning can be detected. In practice, these indicators are useful only where the rate of change in human action is slow enough to detect incipient regime shifts before they occur. But what rates of change in the drivers are slow enough? Further research is needed to determine how rates of change in drivers, in concert with rates of change in ecosystem components and natural disturbance frequencies, affect our ability to detect impending regime shifts.

Even if harvest rate rises slowly, by the time the signals are detectable the harvest rate has been above the critical value of the deterministic skeleton for a long time. This time delay is different from the usual kind of steady-state hysteresis considered in models of alternate stable states. The ecosystem is already poised for catastrophic change. This unstable situation can last a long time because the dynamics are very slow near the switch point. Are ecosystems near stable equilibria, or are they on long slow transients near unstable attractors (Hastings 2004; Van Geest *et al.* 2007)? Empirically, it is not easy to tell unless one has data from ecosystems in both conditions (Ives *et al.* 2003). Return rates should be high for ecosystems near stable attractors, and low for ecosystems on long unstable transients. Long-term field data are needed to compare these alternatives.

Our findings suggest that high-frequency monitoring of ecological variables may provide leading indicators of important regime shifts in ecosystems. The indicators are discernible through trophic cascades in food web compartments that are not directly involved in the regime shift. In particular, standard deviations and the multivariate index are sensitive and easy to measure and compute for many ecosystem variables. These indicators can provide advance warnings when the driver of the regime shift is changing relatively slowly. Climate change, harvest of living resources, nutrient mobilization and changes in land use and hydrology are examples of human-driven changes that are increasing and cause regime shifts for which leading indicators could potentially be devised (MA (Millennium Ecosystem Assessment) 2005). Despite these encouraging modelling results, field tests are needed to evaluate the potential use of these indicators for understanding or managing ecosystems.

## ACKNOWLEDGEMENTS

For helpful comments, we thank Reinette Biggs, Marten Scheffer, Os Schmitz, Egbert van Nes, Tim Wootton and two anonymous referees. We are grateful for financial support from the National Science Foundation, Andrew W. Mellon Foundation and the Vilas Trust.

## REFERENCES


Anderies, J.M., Janssen, M.A. & Walker, B.H. (2002). Grazing management, resilience and dynamics of a fire-driven rangeland system. *Ecosystems*, 5, 23–44.

Berglund, N. & Gentz, B. (2002). Metastability in simple climate models: pathwise analysis of slowly-driven Langevin equations. *Stochastic Dyn.*, 2, 327–356.

Brock, W.A. & Carpenter, S.R. (2006). Variance as a leading indicator of regime shift in ecosystem services. *Ecol. Soc.*, 11, 9. Available at: http://www.ecologyandsociety.org/vol11/iss2/art9/. Last accessed on 29 October 2007.

Carpenter, S.R. (2002). Ecological futures: building an ecology of the long now. *Ecology*, 83, 2069–2083.

Carpenter, S.R. (2003). Regime shifts in lake ecosystems: pattern and variation, Vol. 15. In: *Excellence in Ecology Series*. Ecology Institute, Oldendorf/Luhe, Germany.

Carpenter, S.R. & Brock, W.A. (2004). Spatial complexity, resilience and policy diversity: fishing on lake-rich landscapes. *Ecol. Soc.*, 9, 8. Available at: http://www.ecologyandsociety.org/vol9/iss1/art8 Last accessed on 29 October 2007.

Carpenter, S.R. & Brock, W.A. (2006). Rising variance: a leading indicator of ecological transition. *Ecol. Lett.*, 9, 311–318.

Carpenter, S.R. & Kitchell, J.F. (eds) (1993). *The Trophic Cascade in Lakes*. Cambridge University Press, Cambridge, England.

Carpenter, S.R., Cole, J.J., Hodgson, J.R., Kitchell, J.F., Pace, M.L., Bade, D. *et al.* (2001). Trophic cascades, nutrients and lake productivity: whole-lake experiments. *Ecol. Monogr.*, 71, 163–186.

Clark, J.S., Carpenter, S.R., Barber, M., Collins, S., Dobson, A., Foley, J. *et al.* (2001). Ecological forecasting: an emerging imperative. *Science*, 293, 657–660.

Dutkiewicz, S., Follows, M.J. & Parekh, P. (2005). Interactions of the iron and phosphorus cycles: a three-dimensional model study. *Global Biogeochem. Cycles*, 19, GB1021 (doi: 10.1029/2004GB002342).

Foley, J.A., Coe, M.T., Scheffer, M. & Wang, G. (2003). Regime shifts in the Sahara and Sahel: interactions between ecological and climatic systems in Northern Africa. *Ecosystems*, 6, 524–539.

Folke, C., Carpenter, S.R., Walker, B., Scheffer, M., Elmqvist, T., Gunderson, L. *et al.* (2005). Regime shifts, resilience and biodiversity in ecosystem management. *Ann. Rev. Ecol., Evol. Syst.*, 35, 557–581.

Follows, M.J., Dutkiewicz, S., Grant, S. & Chisholm, S.W. (2007). Emergent biogeography of microbial communities in a model ocean. *Science*, 315, 1843–1846.

Fortin, M.J. & Dale, M.R.T. (2005). *Spatial Analysis: A Guide for Ecologists*. Cambridge University Press, Cambridge, UK.

Groffman, P.M., Baron, J.S., Blett, T., Gold, A.J., Goodman, I., Gunderson, L.H. *et al.* (2006) Ecological thresholds: the key to successful environmental management or an important concept with no practical application. *Ecosystems*, 9, 1–13.

Hastings, A. (2004). Transients: the key to long-term ecological understanding? *Trends Ecol. Evol.*, 19, 39–45.

Holling, C.S. (1973). Resilience and stability of ecological systems. *Ann. Rev. Ecol. Syst.*, 4, 1–23.

Horsthemke, W. & Lefever, R. (1984). *Noise-induced Transitions*. Springer-Verlag, Berlin.

Hsieh, C.-H., Reiss, C.S., Hunter, J.R., Beddington, J.R., May, R.M. & Sugihara, G. (2006). Fishing elevates variability in the abundance of exploited species. *Nature*, 443, 859–862.

Hughes, T.P., Bellwood, D., Folke, C., Steneck, R. & Wilson, J. (2005). New paradigms for supporting the resilience of marine ecosystems. *Trends Ecol. Evol.*, 20, 380–386.

Ives, A.R. & Carpenter, S.R. (2007). Stability and diversity of ecosystems. *Science*, 317, 58–62.

Ives, A.R., Dennis, B., Cottingham, K.L. & Carpenter, S.R. (2003). Estimating community stability and ecological interactions from time-series data. *Ecol. Monogr.*, 73, 301–330.

Jeppesen, E., Sondergaard, M., Sondergaard, M. & Christofferson, K. (eds) (1998). *The Structuring Role of Submerged Macrophytes in Lakes*. Springer-Verlag, Berlin.

Kitchell, J.F. & Carpenter, S.R. (1993). Variability in lake ecosystems: complex responses by the apical predator. In: *Humans as Components of Ecosystems* (eds McDonnell, M.J. & Pickett, S.T.A.). Springer-Verlag, NY, pp. 111–124.

Kleinen, T., Held, H. & Petschel-Held, G. (2003). The potential role of spectral properties in detecting thresholds in the earth system: application to the thermohaline circulation. *Ocean Dyn.*, 53, 53–63.

MA (Millennium Ecosystem Assessment) (2005). *Ecosystems and Human Well-Being. Our Human Planet: Summary for Decision Makers*. Island Press, Washington, DC, Available at: http://www.MAweb.org Last accessed on 29 October 2007.

Mullon, C., Freon, P. & Cury, P. (2005). The dynamics of collapse in world fisheries. *Fish Fish.*, 6, 111–120.

Narisma, G.T., Foley, J.A., Licker, R. & Ramankutty, N. (2007). Abrupt changes in rainfall during the twentieth century. *Geophys. Res. Lett.*, 34, L06710 (doi: 10.1029/2006GL028628).

van Nes, E. & Scheffer, M. (2007). Slow recovery from perturbations as a generic indicator of a nearby catastrophic shift. *Am. Nat.*, 169, 738–747.

Persson, L., Amundsen, P.-A., De Roos, A.M., Klemetsen, A., Knudsen, R. & Primicerio, P. (2007). Culling prey promotes predator recovery – alternative states in a whole-lake experiment. *Science*, 316, 1743–1746.

Peters, D.P.C., Pielke, R.A. Sr, Bestelmeyer, B.T., Allen, C.D., Munson-McGee, S. & Havstad, K.M. (2004). Cross-scale interactions, nonlinearities, and forecasting catastrophic events. *PNAS*, 101, 15130–15135.

Porter, J., Arzberger, P., Hanson, P.C., Kratz, T.K., Gage, S., Williams, T. *et al.* (2005). Wireless sensor networks for ecology. *BioScience*, 55, 561–572.

Reynolds, F. & Stafford-Smith, D.M. (eds) (2002). *Global Desertification: Do Humans Cause Deserts?* Dahlem University Press, Berlin, Germany.

Rietkerk, M., Dekker, S.C., de Ruiter, P.C. & van de Koppel, J. (2004). Self-organized patchiness and catastrophic shifts in ecosystems. *Science*, 305, 1926–1929.

Scheffer, M. (1997). *The Ecology of Shallow Lakes*. Chapman and Hall, London.

Scheffer, M. & Carpenter, S.R. (2003). Catastrophic regime shifts in ecosystems: linking theory to observation. *Trends Ecol. Evol.*, 12, 648–656.

Scheffer, M. & Jeppesen, E. (2007). Regime shifts in shallow lakes. *Ecosystems*, 10, 1–3.

Scheffer, M., Carpenter, S.R., Foley, J., Folke, C. & Walker, B. (2001). Catastrophic shifts in ecosystems. *Nature*, 413, 591–596.

Schmitz, O.J., Kalies, E.L. & Booth, M.G. (2006). Alternative dynamic regimes and trophic control of plant succession. *Ecosystems*, 9, 659–672.

Simenstad, C., Estes, J. & Kenyon, K. (1978). Aleuts, sea otters, and alternative stable state communities. *Science*, 200, 403–411.
Solé, R.V., Manrubia, S.C., Luque, B., Delgado, J. & Bascompte, J. (1996). Phase transitions and complex systems. *Complexity*, 1, 13–26.
Steele, J.H. (1998). Regime shifts in marine ecosystems. *Ecol. Appl.*, 8, S33–S36.
Suding, K.N., Gross, K.L. & Houseman, G.R. (2004). Alternative states and positive feedbacks in restoration ecology. *Trends Ecol. Evol.*, 19, 46–53.
Ursin, E. (1982). Stability and variability in the marine ecosystem. *Dana*, 2, 51–65.
Van Geest, G.J., Coops, H., Scheffer, M. & van Nes, E.H. (2007). Long transients near the ghost of a stable state in eutrophic shallow lakes with fluctuating water levels. *Ecosystems*, 10, 36–46.
Walker, B. & Meyers, J.A. (2004). Thresholds in ecological and social-ecological systems: a developing database. *Ecol. Soc.*, 9, 3. Available at: http://www.ecologyandsociety.org/vol9/iss2/art3 Last accessed on 29 October 2007.
Walters, C. & Kitchell, J.F. (2001). Cultivation/depensation effects on juvenile survival and recruitment: implications for the theory of fishing. *Can. J. Fish. Aquat. Sci.*, 58, 39–50.
Walters, C.J. & Martell, S.J.D. (2004). *Fisheries Ecology and Management*. Princeton University Press, Princeton, NJ.

## SUPPLEMENTARY MATERIAL

The following supplementary material is available for this article:

**Table S1** Parameter values used in the simulations.
**Appendix S1** Estimating the critical point of the deterministic skeleton.
**Figure S1** Histograms from samples of the planktivore stationary distribution at 8 values of $qE$ near the transition point.
**Figure S2** Histograms from samples of the juvenile piscivore stationary distribution at 8 values of $qE$ near the transition point.
**Figure S3** Histograms from samples of the herbivore stationary distribution at 8 values of $qE$ near the transition point.
**Figure S4** Histograms from samples of the phytoplankton stationary distribution at 8 values of $qE$ near the transition point.
**Figure S5** Variance spectra for herbivore biomass.
**Figure S6** Variance spectra for planktivore biomass.
**Figure S7** Standard deviations of the state variables prior to the shift in transient simulations.
**Figure S8** Return rates of the state variables prior to the shift in transient simulations.

The material is available as part of the online article from: http://www.blackwell-synergy.com/doi/full/10.1111/j.1461-0248.2007.01131.x

Please note: Blackwell Publishing are not responsible for the content or functionality of any supplementary materials supplied by the authors. Any queries (other than missing material) should be directed to the corresponding author for the article.

Editor, Tim Wootton
Manuscript received 31 August 2007
First decision made 3 October 2007
Manuscript accepted 10 October 2007

**Supporting Online Materials for**

# Leading Indicators of Trophic Cascades

By
S. R. Carpenter[1*], W. A. Brock[2], J.J. Cole[3], J.F. Kitchell[1] & M.L. Pace[3]

[1]Center for Limnology
University of Wisconsin
Madison, Wisconsin, 53706 USA

[2]Department of Economics
University of Wisconsin
Madison, Wisconsin, 53706 USA

[3]Institute of Ecosystem Studies
P.O. Box AB
Millbrook, NY 12545 USA

*Correspondence: email: srcarpen@wisc.edu; fax 608-265-2340; tel 608-262-8690

**SUPPLEMENTARY MATERIAL**

The following supplementary materials are provided for this manuscript:

**Table S1**. Parameter values used in the simulations.

**Appendix S1**. Estimating the critical point of the deterministic skeleton

**Figure S1**. Histograms from samples of the planktivore stationary distribution at 8 values of qE near the transition point.

**Figure S2**. Histograms from samples of the juvenile piscivore stationary distribution at 8 values of qE near the transition point.

**Figure S3**. Histograms from samples of the herbivore stationary distribution at 8 values of qE near the transition point.

**Figure S4**. Histograms from samples of the phytoplankton stationary distribution at 8 values of qE near the transition point.

**Figure S5**. Variance spectra for herbivore biomass.

**Figure S6**. Variance spectra for planktivore biomass.

**Figure S7**. Standard deviations of the state variables prior to the shift in transient simulations.

**Figure S8**. Return rates of the state variables prior to the shift in transient simulations.

Table S1. Parameter values used for the simulations.

| Symbol | value | units | interpretation | source |
|---|---|---|---|---|
| $\alpha$ | 0.3 | g $g^{-1}$ | Conversion of consumed phytoplankton phosphorus to zooplankton phosphorus | Fit to data of Carpenter et al. 2001 |
| $\sigma_F$, $\sigma_H$, $\sigma_P$ | 0.1 | Same as F, H and P, respectively | Standard deviation of stochastic process | Arbitrary |
| A2biom | 0.2 | kg/fish | Convert densities to kg $ha^{-1}$ | Fit to data of Carpenter et al. 2001 |
| $c_{FA}$ | 0.3 | $t^{-1}$ $A^{-1}$ | Consumption coefficient of planktivores by adult piscivores | Fit to data of Carpenter et al. 2001 |
| $c_{HF}$ | 0.1 | $t^{-1}$ $F^{-1}$ | Consumption rate of zooplankton by planktivore | Fit to data of Carpenter et al. 2001 |
| $c_{JA}$ | 0.001 | $t^{-1}$ $A^{-1}$ | Consumption coefficient of juvenile piscivores by adult piscivores | Fit to data of Carpenter et al. 2001 |
| $c_{JF}$ | 0.5 | $t^{-1}$ $F^{-1}$ | Consumption coefficient of juvenile piscivores by planktivores | Fit to data of Carpenter et al. 2001 |
| $c_{PH}$ | 0.25 | $t^{-1}$ $H^{-1}$ | Consumption rate of phytoplankton by zooplankton | Fit to data of Carpenter et al. 2001 |
| $D_F$ | 0.1 | $t^{-1}$ | Diffusion parameter for planktivores | Fit to data of Carpenter et al. 2001 |
| $D_H$ | 0.5 | $t^{-1}$ | Zooplankton diffusion parameter | Fit to data of Carpenter et al. 2001 |
| DOC | 5 | G m-3 | DOC concentration | Typical value for our experimental lakes (Carpenter et al. 2001) |
| F2biom | 1 | kg/(500 fish) | Convert densities to kg $ha^{-1}$ | Fit to data of Carpenter et al. 2001 |
| f | 2 | $J_{t+1} / (A_{tl} + J_{tl})$ | Fecundity of adult piscivore | Fit to data of Carpenter et al. 2001 |
| Fo | 100 | F | Refuge density of planktivores | Fit to data of Carpenter et al. 2001 |
| h | 8 | $t^{-1}$ | Refuging parameter for juvenile piscivores | Fit to data of Carpenter et al. 2001 |
| Ho | 1 | H | Refuge biomass | Fit to data of Carpenter et al. 2001 |
| $I_0$ | 300 | $\mu$Eins $m^{-2}$ $s^{-1}$ | Surface irradiance | Typical daily average for summer on Sparkling Lake (NTL-LTER) |

| | | | | |
|---|---|---|---|---|
| $I_Z$ | - | μEins $m^{-2}$ $s^{-1}$ | irradiance at depth Z ($I_0$ is sometimes a parameter; otherwise $I_Z$ is a variable) | - |
| J2biom | 0.05 | kg/(10 fish) | Convert densities to kg $ha^{-1}$ at the end of a maturation interval | Fit to data of Carpenter et al. 2001 |
| $k_{DOC}$ | 0.0514 | $m^2$ $g^{-1}$ | light extinction by DOC | Carpenter et al. 1998 |
| $k_{grow}$ | 0.012 | (μEins $m^{-2}$ $s^{-1}$)$^{-1}$ | phytoplankton growth in response to irradiance | Follows et al. 2007 |
| $k_{inhib}$ | 0.004 | (μEins $m^{-2}$ $s^{-1}$)$^{-1}$ | light inhibition of phytoplankton | Follows et al. 2007 |
| $k_o$ | 0.0213 | $m^{-1}$ | light extinction by water molecules | Carpenter et al. 1998 |
| $k_P$ | 0.0177 | $m^2$ $mg^{-1}$ | light extinction by phytoplankton measured as P or chlorophyll (1:1 ratio from Reynolds 1997) | Carpenter et al. 1998 |
| L | 0.6 | mg $m^{-2}$ $t^{-1}$ | Phosphorus load | Approximately twice the baseline value, representing a mildly enriched experimental lake (Carpenter et al. 2001) |
| m | 0.1 | $t^{-1}$ | per capita mortality of phytoplankton | Follows et al. 2007 |
| qE | varied | $t^{-1}$ | Harvest rate (catchability times fishing effort) | |
| $r_P$ | 3 | $m^2$ $mg^{-1}$ | Phytoplankton growth parameter per unit phosphorus load | Fit to data of Carpenter et al. 2001 |
| s | 0.5 | $t^{-1}$ | Overwinter survivorship of piscivores | Fit to data of Carpenter et al. 2001 |
| v | 1 | $t^{-1}$ | Vulnerability parameter for juvenile piscivores | Fit to data of Carpenter et al. 2001 |
| $Z_{mix}$ | 4 | m | Mixed layer depth | Typical value for our experimental lakes (Carpenter et al. 2001) |

References for Table S1

Carpenter, S.R., J.J. Cole, J.F. Kitchell, and M.L. Pace. 1998. Impact of dissolved organic carbon, phosphorus and grazing on phytoplankton biomass and production in experimental lakes. Limnology and Oceanography 43: 73-80.

Carpenter, S.R., J.J. Cole, J.R. Hodgson, J.F. Kitchell, M.L. Pace,D. Bade, K.L. Cottingham, T.E. Essington, J.N. Houser and D.E. Schindler. 2001. Trophic cascades, nutrients and lake productivity: whole-lake experiments. Ecological Monographs 71: 163-186.

Dutkiewicz, S., M.J. Follows and P. Parekh. 2005. Interactions of the iron and phosphorus cycles: A three-dimensional model study. Global Biogeochemical Cycles 19, GB 1021. doi: 10.1029/2004GB002342, 2005.

Follows, M.J., S. Dutkeiwicz, S. Grant and S.W. Chisholm. 2007. Emergent biogeography of microbial communities in a model ocean. Science 315: 1843-1846.

NTL-LTER. Data base of the North Temperate Lakes Long-Term Ecological Research Program. http://lter.limnology.wisc.edu

Reynolds, C.S. 1997. *Vegetation Processes in the Pelagic: A Model for Ecosystem Theory*. Exellence in Ecology Vol. 9, Ecology Institute, Oldendorf/Luhe, Germany.

Appendix 1. Estimating the switch point for the piscivores.

The deterministic skeleton of the model is the dynamic equations with no added noise. In equations 1, 2, 3, 7 and 8 of the main text, $\sigma_F$, $\sigma_H$ and $\sigma_P$ were set equal to zero to obtain the deterministic skeleton.

The critical points of the deterministic skeleton are useful for interpreting the simulations, even though the deterministic critical points need not correspond to the moments or extrema of the stationary distributions of the stochastic model (Horsthemke and Lefever 1984). Here we report a numerical estimate of the value of qE where the upper steady state for piscivores disappears.

The usual procedure for solving for a bifurcation point for a system of equations

$$X(t+1) - X(t) = f[X(t),\theta]$$

where $\theta$ is scalar and X is an n-dimensional vector is to solve the equation

$$0 = f[X^*(\theta), \theta]$$

for the steady state $X^*(\theta)$, assuming it is unique in the domain where we are working. Then calculate the n x n Jacobian matrix $\partial f/\partial X$ and evaluate it at $[X^*(\theta), \theta]$. Call this $J^*(\theta)$. Evaluate the n eigenvalues of $I+J^*(\theta)$ for each $\theta$ and find $\theta_C$ such that the largest modulus eigenvalue is on the boundary of the unit circle in the complex plane. See Kuznetsov (1995, Chapter 4) for the details of bifurcation analysis for one-parameter bifurcations in discrete time dynamical systems.

Our system can be converted to difference equations where the time step is one maturation interval by the procedure described in the main text. We could conduct a bifurcation analysis by starting at $\theta \equiv qE = 0$ where all eigenvalues of the 5 x 5 matrix $I+J^*(\theta)$ are inside the unit circle, and then gradually increase qE until a value is reached so that the largest value eigenvalue exits the unit circle on the complex plane. However, this is numerical analysis is difficult due to near-singularity of $I+J^*(\theta)$ near equilibrium. Therefore, we substituted the following approximate procedure. Our approximate procedure yields an estimate of the value of qE at which the piscivore population collapses. We do not claim that this switch point is the same as a formal bifurcation analysis, but simulations reported in this paper and the numerical analyses shown below indicate that the switch point is very close to the value of qE at which the trophic cascade is triggered in the deterministic skeleton.

We focus on the dynamics of A and F. Define $\Delta(X) \equiv X_{t+1} - X_t$ where X is one of the state variables and t to t+1 represents the time between the beginnings of two successive maturation intervals.

In the deterministic skeleton, note from equation 6 of the main text that $\Delta(J(t)) = f\, s\, \Delta(A(t))$ so if A is at equilibrium then J is at equilibrium (i.e. if $\Delta(A) = 0$ then $\Delta(J) = 0$). Also, note that the dynamics of H and P depend on F, but the dynamics of F and A do not depend on H and P. Finally, note that within a maturation interval starting at $A_t$ the dynamics of A are given by $A_i =$

$A_t \exp(-qE\, i)$. Thus the dynamics of F within a maturation interval ($t < i < t+1$) in the deterministic skeleton simplify to

$$\frac{dF}{di} = D_F (F_R - F) - c_{FA} F A_t \exp(-qE\, i)$$

Thus dynamics of F depend only on F, time i within the maturation interval, and constants.

Figure S2.1 Rate Δ(A) versus A density. Colors denote values of qE. For these plots, F was set to 1.69, near the solution found numerically in the text of Appendix S2.

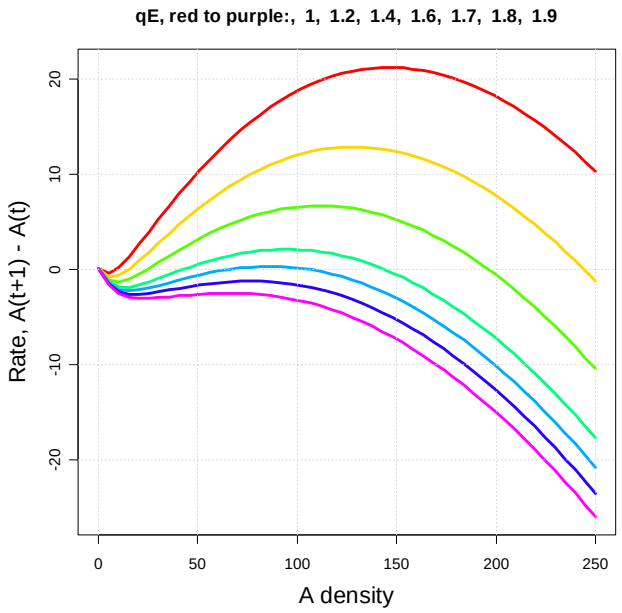


If we plot Δ(A) versus A (the stock of adult fish), we see a S-shaped curve that crosses Δ(A)=0 three times if qE is small and once if qE is large (Fig. S2.1). These crossing points are equilibria for A. The lower and upper equilibria are stable, and the middle one is unstable.

If qE is raised slowly, the S-curve tilts downward on the right. The larger (right hand) stable equilibrium for A becomes smaller and comes closer to the middle, unstable equilibrium value. At a switch point value of qE, the upper equilibrium for A disappears as the S-curve tilts below the line where the y-axis value is zero.

Numerically, these conditions are met by finding the values of qE, A and F (the planktivore) that satisfy the equations

$$\Delta(A) = 0$$
$$\partial[\Delta(A)]/\partial A = 0 \qquad [10, 11, 12,]$$
$$\Delta(F) = 0$$

Using the box-constrained quasi-Newton method in R, we get the following values for qE, A and F at the switch point: 1.7169, 85.8017, 1.6907. Using the Nelder-Mead method in R, we get 1.7169, 85.7777, 1.6911, essentially the same answer.

References for Appendix S2

Horsthemke, W. and R. Lefever. 1984. *Noise-Induced Transitions*. Springer-Verlag, Berlin.

Kuznetsov, Y.A. 1995. *Elements of Applied Bifurcation Theory*. Springer-Verlag, Berlin.

Figure S1. Histograms from samples of the planktivore stationary distribution at 8 values of qE near the transition point. For each histogram, a simulation was initialized near the critical point values of the state variables, run for 10,240 time steps, and then data for the histogram were collected for 2048 time steps.

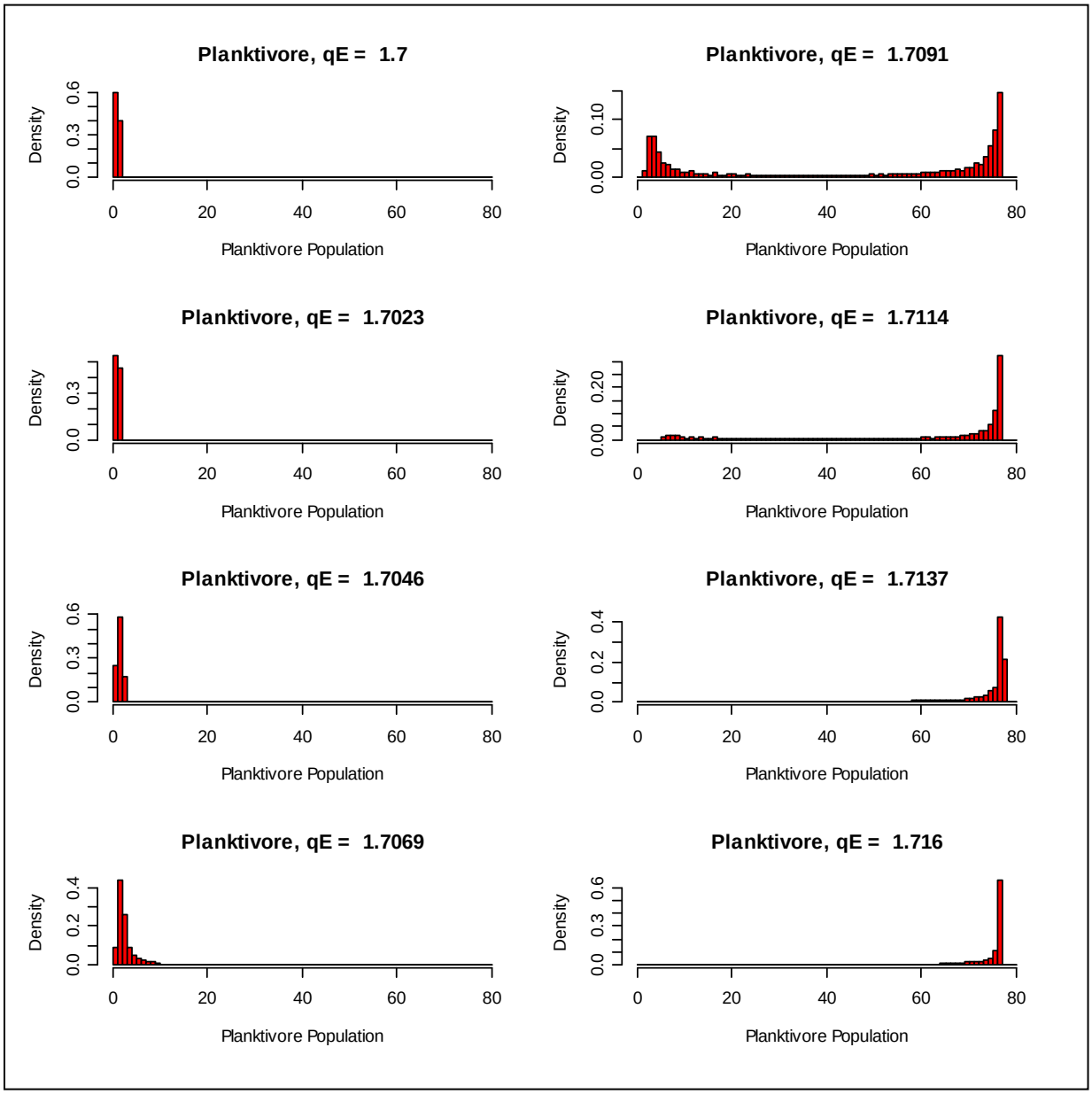

Figure S2. Histograms from samples of the juvenile piscivore stationary distribution at 8 values of qE near the transition point. For each histogram, a simulation was initialized near the critical point values of the state variables, run for 10,240 time steps, and then data for the histogram were collected for 2048 time steps.

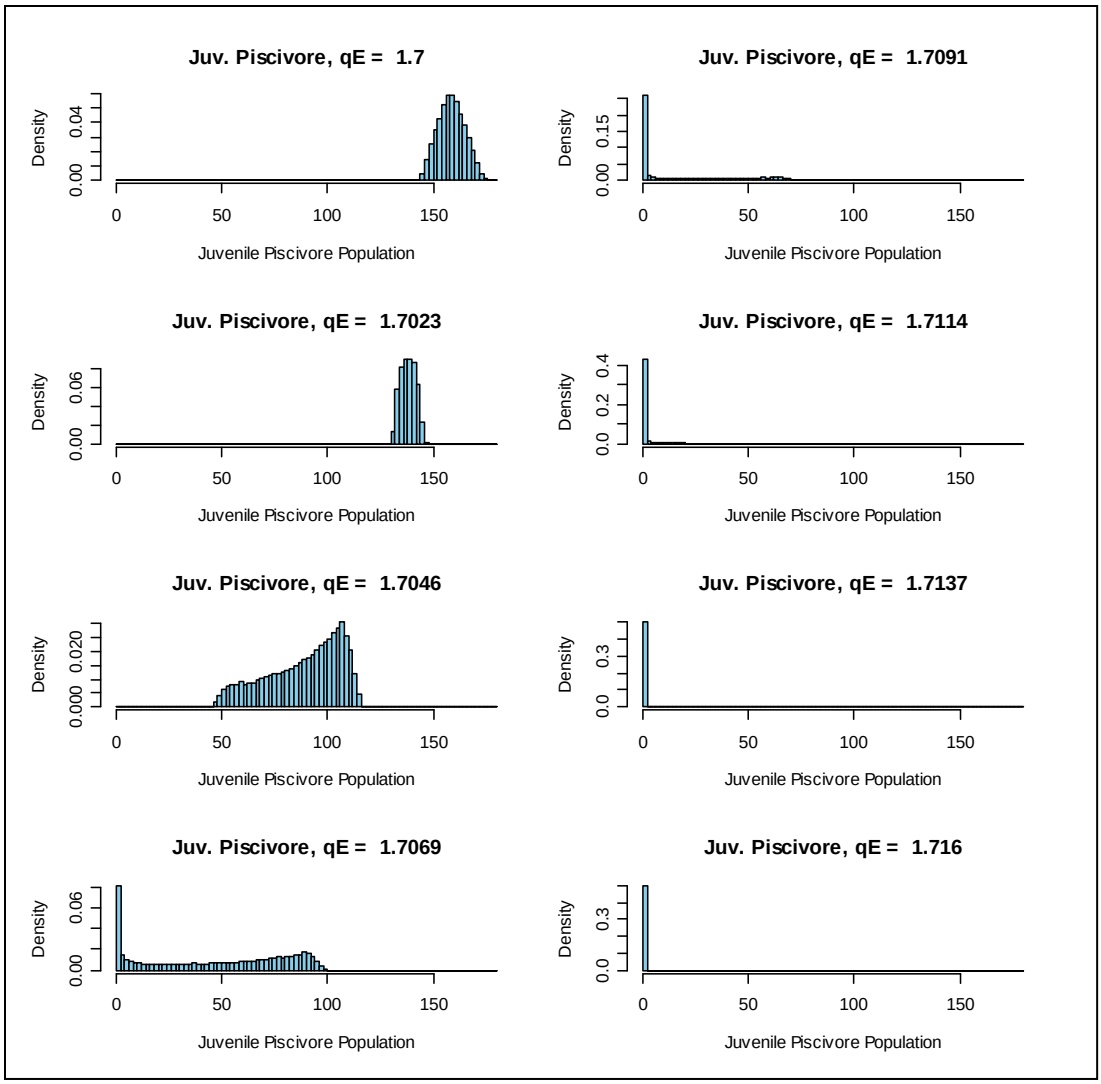

Figure S3. Histograms from samples of the herbivore stationary distribution at 8 values of qE near the transition point. For each histogram, a simulation was initialized near the critical point values of the state variables, run for 10,240 time steps, and then data for the histogram were collected for 2048 time steps.

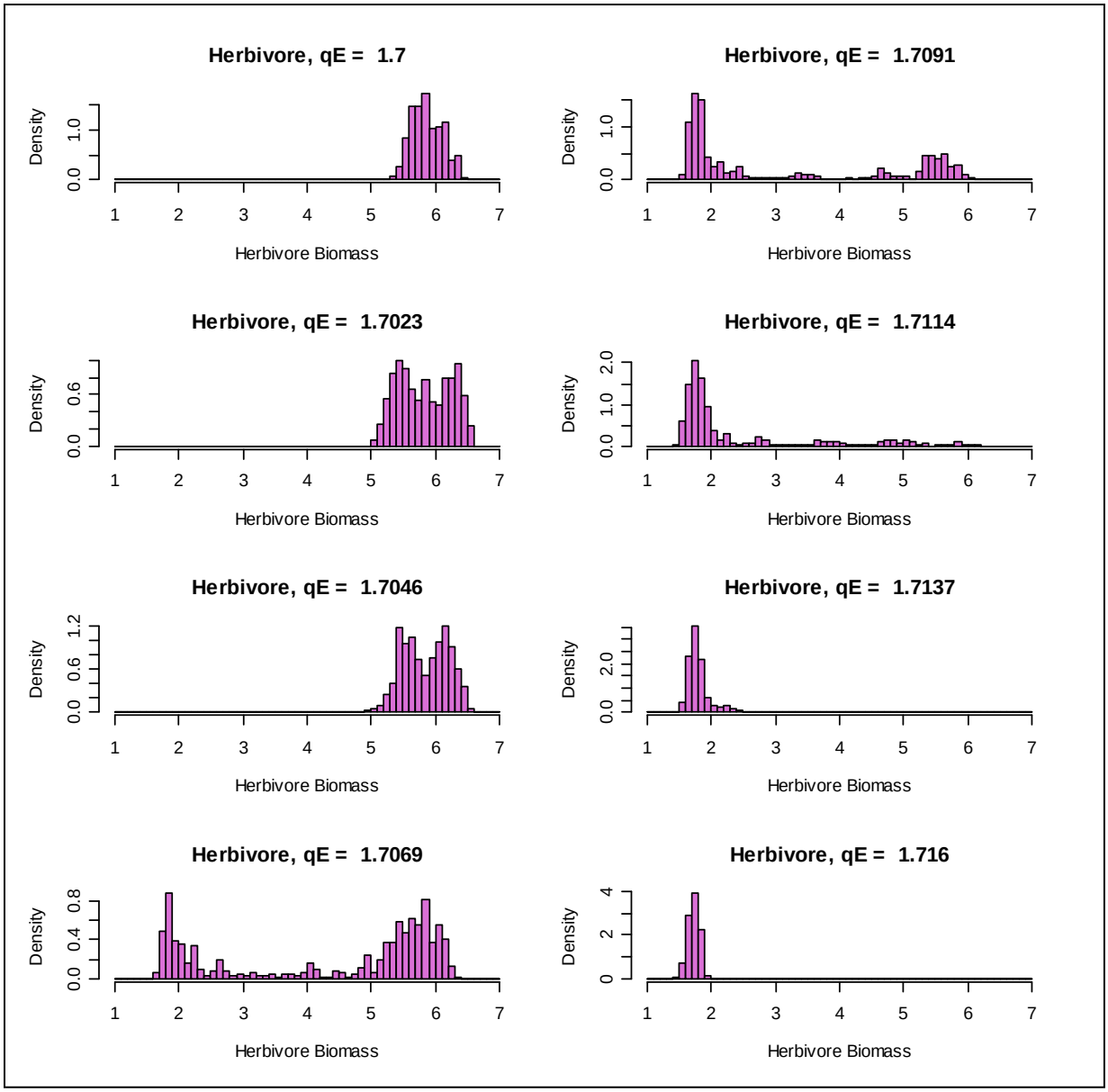

Figure S4. Histograms from samples of the phytoplankton stationary distribution at 8 values of qE near the transition point. For each histogram, a simulation was initialized near the critical point values of the state variables, run for 10,240 time steps, and then data for the histogram were collected for 2048 time steps.

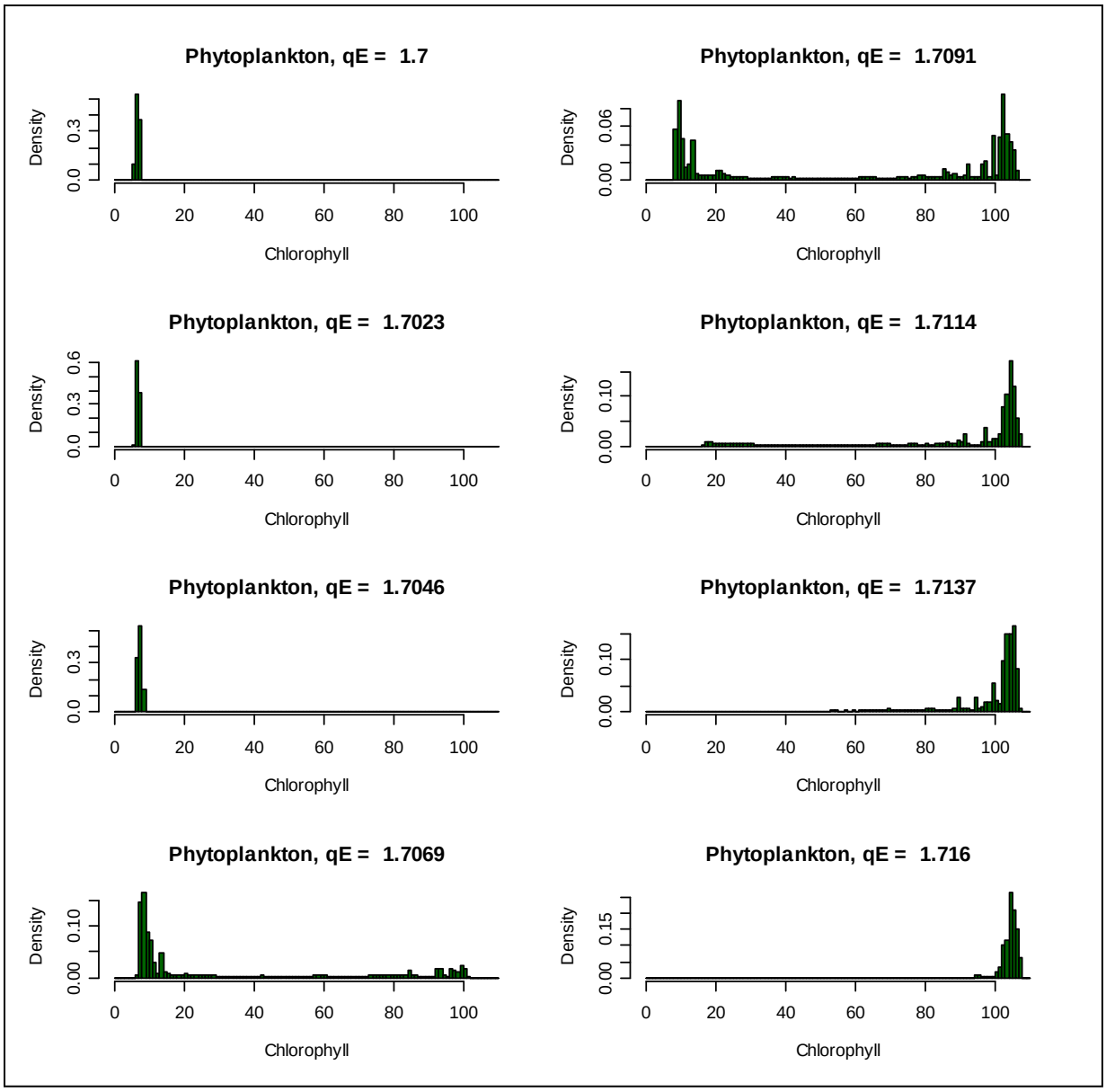

Figure S5. Variance spectra for herbivore biomass. The surface depicts log spectral density (contours) versus log frequency (horizontal axis; log(one maturation interval) = -3.47) and qE (vertical axis) for herbivore biomass. Starting with the lowest spectral density in blue, log spectral density rises from -11 to +5 through green, yellow, dark tan and light tan as the highest spectral density.

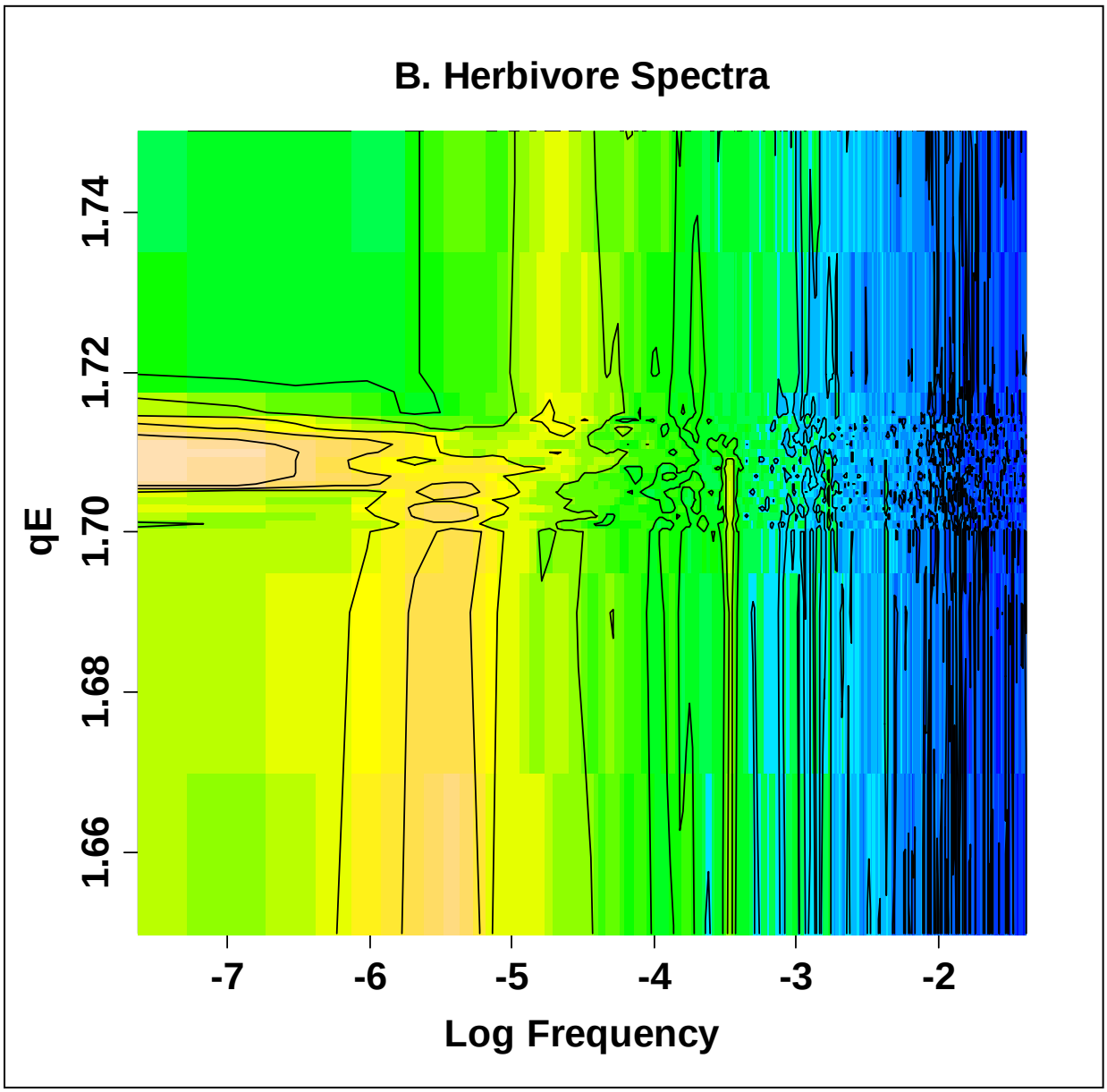

Figure S6. Variance spectra for planktivore biomass. The surface depicts log spectral density (contours) versus log frequency (horizontal axis; log(one maturation interval) = -3.47) and qE (vertical axis) for planktivore biomass. Starting with the lowest spectral density in blue, log spectral density rises from -11 to +11 through green, yellow, dark tan and light tan as the highest spectral density.

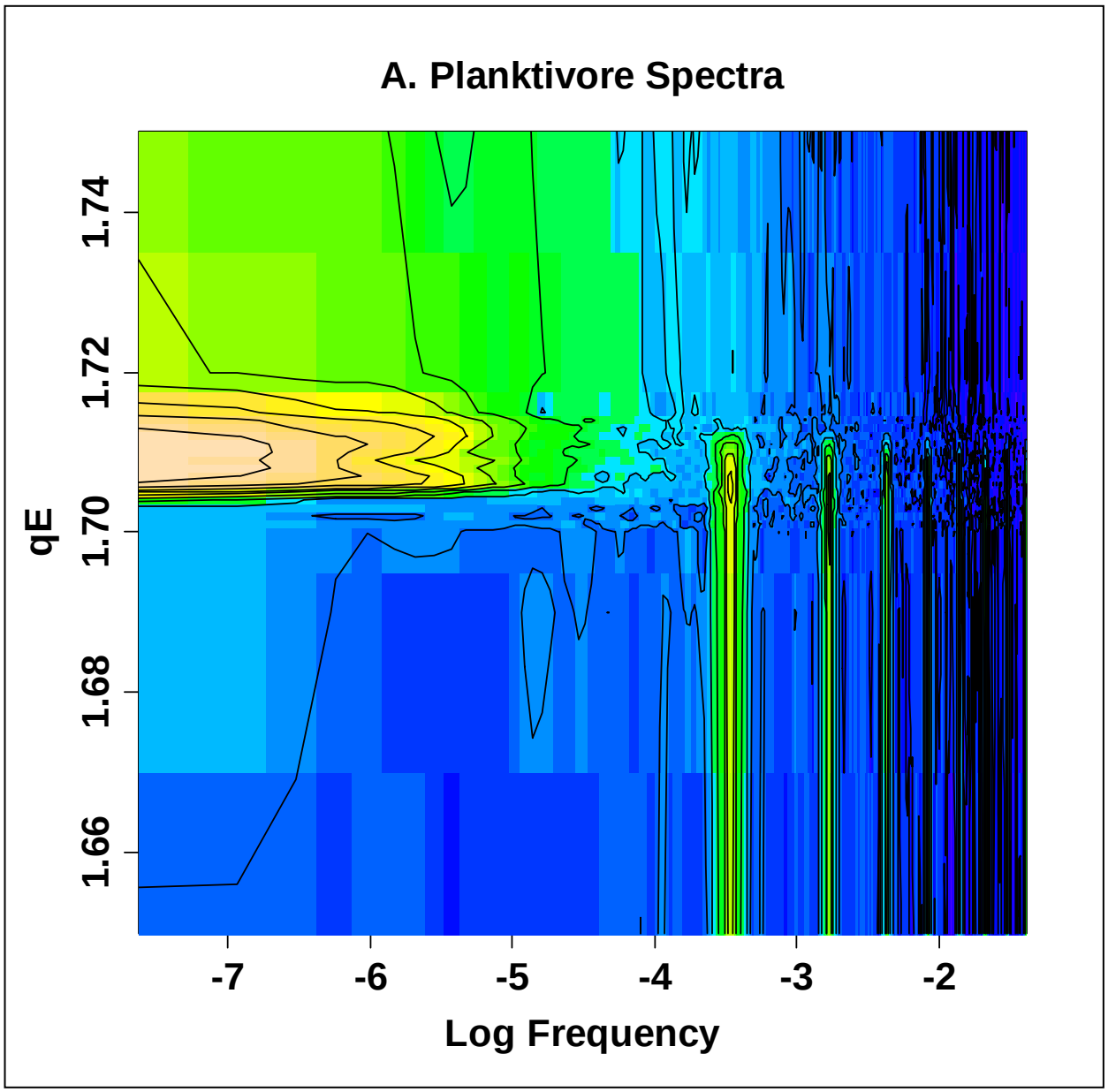

Figure S7. Standard deviations of the state variables prior to the shift in transient simulations. Over 96,000 time steps qE was raised linearly from 1.5 to 2. Standard deviations were calculated over time intervals of 32 steps, the maturation time of the piscivore. Zero denotes the time step of most rapid increase of the planktivore.

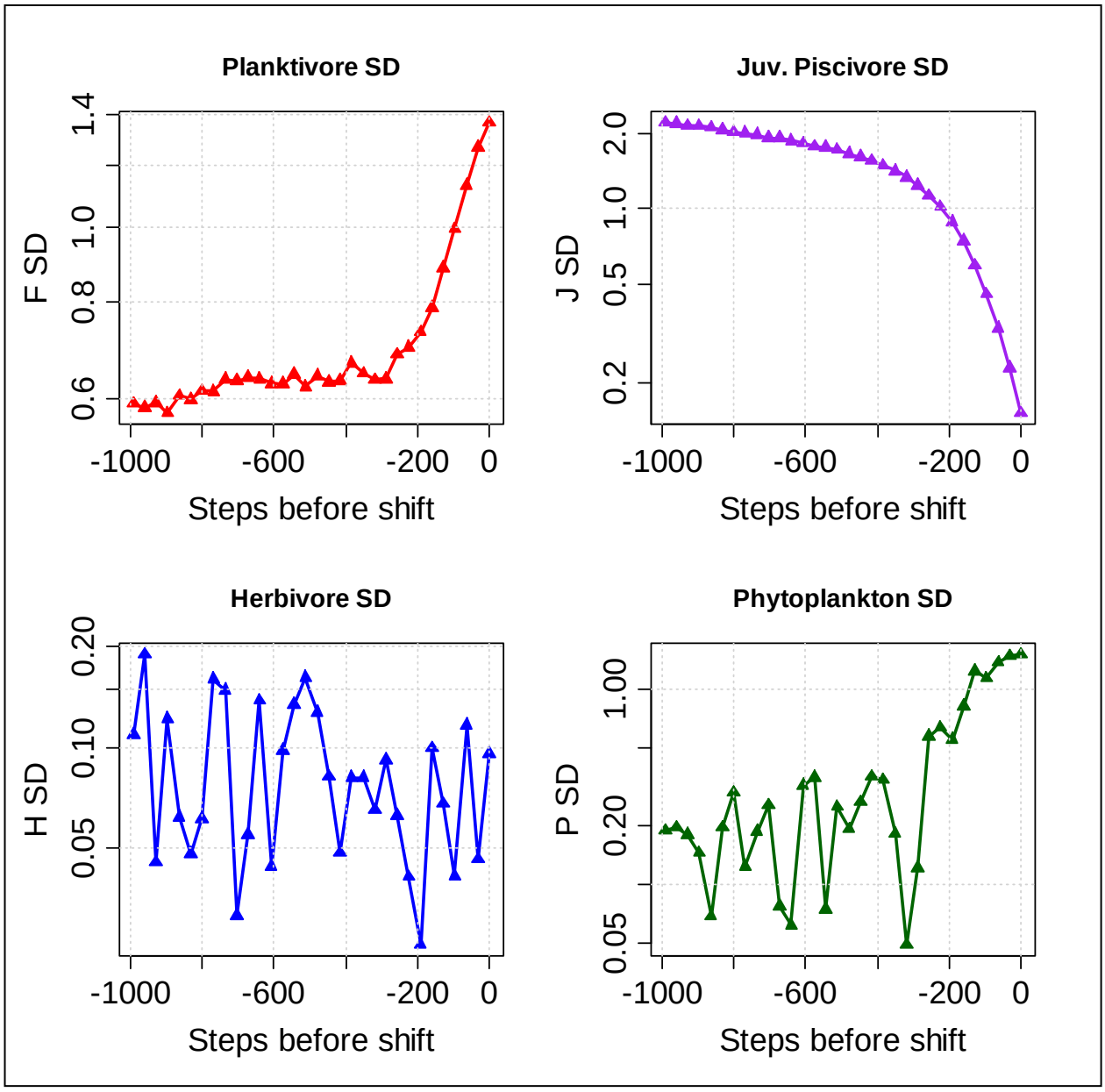

Figure S8. Return rates of the state variables prior to the shift in transient simulations. Over 96,000 time steps qE was raised linearly from 1.5 to 2. Return rates were estimated by the method described in the text over time intervals of 32 steps, the maturation time of the piscivore. Zero denotes the time step of most rapid increase of the planktivore.